

Histone deacetylase inhibitors correct the cholesterol storage defect in most Niemann-Pick C1 mutant cells^S

Nina H. Pipalia,^{1,*} Kanagaraj Subramanian,^{1,†} Shu Mao,^{1,*} Harold Ralph,^{*} Darren M. Hutt,[†] Samantha M. Scott,[†] William E. Balch,^{2,†} and Frederick R. Maxfield^{2,*}

Department of Biochemistry,^{*} Weill Cornell Medical College, New York, NY 10065; and Department of Chemical Physiology and Cell and Molecular Biology,[†] The Skaggs Institute for Chemical Biology, The Scripps Research Institute, La Jolla, CA, 92037

ORCID IDs: 0000-0002-7619-7351 (N.H.P.), 0000-0003-4396-8866 (F.R.M.)

Abstract Niemann-Pick C (NPC) disease is an autosomal recessive disorder that leads to excessive storage of cholesterol and other lipids in late endosomes and lysosomes. The large majority of NPC disease is caused by mutations in NPC1, a large polytopic membrane protein that functions in late endosomes. There are many disease-associated mutations in NPC1, and most patients are compound heterozygotes. The most common mutation, NPC1^{I1061T}, has been shown to cause endoplasmic reticulum-associated degradation of the NPC1 protein. Treatment of patient-derived NPC1^{I1061T} fibroblasts with histone deacetylase inhibitors (HDACis) vorinostat or panobinostat increases expression of the mutant NPC1 protein and leads to correction of the cholesterol storage. Here, we show that several other human NPC1 mutant fibroblast cell lines can also be corrected by vorinostat or panobinostat and that treatment with vorinostat extends the lifetime of the NPC1^{I1061T} protein. To test effects of HDACi on a large number of NPC1 mutants, we engineered a U2OS cell line to suppress NPC1 expression by shRNA and then transiently transfected these cells with 60 different NPC1 mutant constructs. **The mutant NPC1 did not significantly reduce cholesterol accumulation, but approximately 85% of the mutants showed reduced cholesterol accumulation when treated with vorinostat or panobinostat.**—Pipalia, N. H., K. Subramanian, S. Mao, H. Ralph, D. M. Hutt, S. M. Scott, W. E. Balch, and F. R. Maxfield. **Histone deacetylase inhibitors correct the cholesterol storage defect in most Niemann-Pick C1 mutant cells.** *J. Lipid Res.* 2017. 58: 695–708.

Supplementary key words NPC1 • cellular cholesterol • lipid transport • inborn errors of metabolism • drug therapy • cholesterol trafficking

This work was supported by National Institute of Neurological Disorders and Stroke Grant R01-NS092653; National Institute of Diabetes and Digestive and Kidney Diseases Grant R37DK27083; and grants from the Ara Parseghian Medical Research Foundation (to F.R.M.). The content is solely the responsibility of the authors and does not necessarily represent the official views of the National Institutes of Health.

Manuscript received 22 September 2016 and in revised form 24 January 2017.

*Published, JLR Papers in Press, February 13, 2017
DOI 10.1194/jlr.M072140*

Copyright © 2017 by the American Society for Biochemistry and Molecular Biology, Inc.

This article is available online at <http://www.jlr.org>

Lipoprotein-derived cholesterol is normally transported out of late endosomes and lysosome (LE/Ly) by a process that requires the Niemann-Pick C1 (NPC1) and NPC2 proteins (1, 2). A current model (3) suggests that cholesterol, which is a product of the hydrolysis of cholesteryl esters by lysosomal acid lipase, is first transferred to NPC2, a cholesterol binding protein. The cholesterol can then be transferred to the N-terminal domain of NPC1, a LE/Ly membrane protein with 13 transmembrane segments (4). This model is supported by recent structural studies of NPC1 (5, 6) and NPC2 bound to the middle luminal domain of NPC1 (7). Cholesterol finally leaves the LE/Ly by a process that is not well understood. In cells with mutations in NPC1 or NPC2, cholesterol and other lipids accumulate in the LE/Ly. Cells with these mutations also show multiple defects in lipid and protein trafficking (8, 9).

Defects in NPC1 or NPC2 in humans lead to an autosomal recessive lysosomal storage disease, Niemann-Pick C (NPC) disease, which causes pathology in multiple tissues, but especially in the central nervous system (10, 11). A high fraction of patients with NPC disease die of neurological complications before the age of 25 (10). In addition to cholesterol, other lipids, including glycosphingolipids, accumulate in the LE/Ly of patient cells. There are currently no effective treatments for NPC disease approved by the

Abbreviations: AcLDL, acetylated LDL; eGFP, enhanced green fluorescent protein; ERAD, endoplasmic reticulum-associated degradation; FDA, Food and Drug Administration; GFP, green fluorescent protein; HDACi, histone deacetylase inhibitor; HPBCD, hydroxypropyl- β -cyclodextrin; LAMP1, lysosomal associated membrane protein 1; LE/Ly, late endosomes and lysosome; LSO, lysosomal storage organelle; NPC, Niemann-Pick C; PFA, paraformaldehyde; P/S, penicillin/streptomycin; SRA, scavenger receptor type A; UTR, untranslated region; WT-V, WT variant.

¹N. H. Pipalia, K. Subramanian, and S. Mao contributed equally to this work.

²To whom correspondence should be addressed.

email: firmaxfie@med.cornell.edu (F.R.M.); webalch@scripps.edu (W.E.B.)

^SThe online version of this article (available at <http://www.jlr.org>) contains a supplement.

Food and Drug Administration (FDA). Miglustat, an inhibitor of glycosphingolipid synthesis (12), shows some beneficial effects and is approved for use in several countries (13, 14). Treatment of mice and cats with hydroxypropyl- β -cyclodextrin (HPBCD) has been shown to effectively reduce the storage of cholesterol and other lipids in cells and to ameliorate symptoms (15–17). HPBCD does not cross the blood-brain barrier, so in cats and humans it needs to be injected directly into the CNS. Early stage clinical trials of HPBCD have been carried out in humans (18).

In a previous study (19), we showed that histone deacetylase inhibitors (HDACis), including vorinostat (also called suberoylanilide hydroxamic acid, or SAHA) and panobinostat (LBH589), are remarkably effective in correcting the NPC1 phenotype in human fibroblast cells that have an *NPC1*^{I1061T} mutation. The pharmacological profile was most consistent with the effects being attributed to inhibition of HDACs 1, 2, or 3 (20). Treatment of patient-derived fibroblasts with HDACi reduced the accumulation of cholesterol in lysosomal storage organelles (LSOs) and restored other aspects of cholesterol homeostasis, including normal processing of sterol regulatory element-binding protein 2 and reduction of the expression of LDL receptors (19, 21). HDACi treatment did not correct the cholesterol storage defect of patient-derived cells expressing *NPC2* mutations (19), indicating that the HDACis do not bypass the need for the NPC1/NPC2 transport system as HPBCD does (22). This indicated that the HDACi might work by allowing the mutant NPC1 proteins to function sufficiently well to correct the cholesterol transport out of LSOs. Vorinostat and panobinostat do enter the CNS, although the levels achieved in the brain are much lower than in the plasma (20, 23, 24). Nevertheless, there is some evidence that vorinostat has effects on tumors in brains (23). Some other HDACis do cross the blood-brain barrier more efficiently and have been shown to have neurological effects in animal studies (25).

The mechanism by which HDACi might restore the function of mutant NPC1 proteins has not been determined. It has been observed that there is more rapid degradation of the NPC1^{I1061T} protein as compared with WT NPC1 protein, and it was proposed that this is because of enhanced endoplasmic reticulum-associated degradation (ERAD) of the mutant protein (26). Treatment of cells expressing NPC1^{I1061T} with HDACi such as panobinostat or vorinostat increased the expression of the mutant NPC1 protein (19). Correction of the NPC phenotype would require that this mutant protein retains adequate functional capability and that a sufficient amount is delivered to the LE/Ly. Other data are consistent with the hypothesis that some mutant NPC1 proteins can function in LE/Ly if they are delivered to those organelles. Simply overexpressing NPC1^{I1061T} in mutant cells leads to partial correction of the phenotype (26). Some indirect treatments also increase the abundance of NPC1 and lead to correction of the phenotype in cultured cells. These include treatment with ryanodine receptor antagonists (27), treatment with oxysterols that bind to NPC1 (28), or reduced expression of TMEM97, an NPC1-binding protein (29). These studies

have indicated that alterations in the proteostasis environment (30–32) by various mechanisms leads to reduced degradation of mutant forms of NPC1. As described here, we found that treatment of some NPC1 mutant cells with vorinostat led to a longer lifetime of the NPC1^{I1061T} protein and increased delivery of the protein to LE/Ly.

A mouse knock-in model of NPC1^{I1061T} has been described recently, and mouse embryo fibroblasts from these mice respond to vorinostat similarly to the human *NPC1*^{I1061T} fibroblasts (33). Another recent study in *Npc1*^{nmj164} mice, which have a D1005G mutation in the *Npc1* protein, reported that a combination therapy with vorinostat, HPBCD, and polyethylene glycol led to slowed neuronal degeneration and improved lifespan in *Npc1*^{nmj164} mutant animals (34).

Approximately 95% of NPC cases are due to mutations in the NPC1 protein, and the *NPC1*^{I1061T} mutation, which occurs in approximately 15–20% of NPC1 patients, is the most commonly observed mutation (35, 36). However, more than 300 different *NPC1* mutations have been observed that are known to be or are likely to be pathogenic (10, 37). It would be very difficult to test drug treatments in hundreds of different human NPC1 mutant fibroblast cell lines, and the large number of compound heterozygous mutations would make it nearly impossible to evaluate the ability of HDACis to correct a specific mutation. In order to evaluate the effectiveness of HDACis as a potential therapy for NPC patients, we developed an efficient screening system using an engineered cell line. Human U2OS osteosarcoma cells were stably transfected with scavenger receptor type A (SRA), and the endogenous NPC1 expression in the cells was stably silenced with an shRNA. The U2OS-SRA-shNPC1 cells were then transiently transfected with a bicistronic vector expressing green fluorescent protein (GFP) (to identify transfected cells) and one of 60 *NPC1* mutations found in patients. This system was used to test the effect of HDACi treatments on multiple NPC1 mutations simultaneously. After treatment with vorinostat or panobinostat, a high fraction of NPC1 mutant proteins were effective in reducing cholesterol accumulation. This suggests that HDACi therapy might be effective for a large majority of NPC1 patients. Because vorinostat and panobinostat are FDA-approved drugs for treatment of some cancers, and other HDACis have been in large scale clinical trials, HDACis may be considered as a potential therapy for NPC1 disease (20).

MATERIALS AND METHODS

Reagents

Gibco® McCoy's 5A medium (Gibco, Tokyo, Japan), MEM, FBS, HBSS, penicillin/streptomycin (P/S), Geneticin (G418), Alexa Fluor 546, Cy5 goat anti-rat (A10525), and Alexa Fluor 546 goat anti-rabbit and Alexa Fluor 488 goat anti-rat antibody, 1,1'-dioctadecyl-3,3',3''-tetramethylindocarbocyanine perchlorate [DiI18 (3)] were purchased from Invitrogen Life Technologies Corp. (Carlsbad, CA). Effectene Transfection Reagent Kit and DNA purification kit was purchased from Qiagen Inc. (Valencia, CA).

HDACis (vorinostat and panobinostat) were stocked at a concentration of 5 mM in DMSO and stored at -20°C . Vorinostat and panobinostat were a generous gift from Dr. Paul Helquist (University of Notre Dame, South Bend, IN). Acetylated LDL (AcLDL) was prepared by acetylation of LDL with acetic anhydride (38). Alexa Fluor 546-labeled human LDL was prepared as described (39, 40). Rabbit polyclonal anti-NPC1 antibody and rabbit polyclonal anti-lysosomal associated membrane protein 1 (anti-LAMP1) antibody (ab24170) were purchased from Abcam (Cambridge, MA). A rat monoclonal anti-NPC1 antibody has been described previously (32). The specificity of the rabbit anti-NPC1 antibody was verified by immunostaining U2OS-SRA-shNPC1 cells, which are stably silenced for NPC1 expression in parallel with WT U2OS cells. In WT U2OS cells, NPC1 staining was observed in punctate LE/Ly, but no staining was observed in U2OS-SRA-shNPC1 cells, indicating that antibody specifically binds to NPC1 protein in cells (supplemental Fig. S1). Similar specificity of labeling was observed for the rat monoclonal anti-NPC1. All other chemicals, including DMSO, 99% fatty-acid free BSA, filipin, paraformaldehyde (PFA), and HEPES were purchased from Sigma-Aldrich (St. Louis, MO). Draq5 was from Biostatus (Leicestershire, UK). Metamorph image-analysis software was from Molecular Devices (Downington, PA).

Human fibroblast cells

Human NPC1 fibroblasts GM05659, GM18453 (homozygous NPC1 mutant *I1061T*), and GM03123 (heterozygous NPC1 mutations *P237S* and *I1061T*) were from Coriell Institute (Camden, NJ). [The *P237S* allele has been found recently to be in linkage with a pathogenic splice mutation that may be responsible for its defect (F.D. Porter, unpublished observations)]. Patient-derived mutant NPC1 skin fibroblasts were from Forbes Porter's laboratory at the National Institutes of Health (Bethesda, MD) as listed in **Table 1**. All human skin fibroblasts were maintained in MEM supplemented with 10% FBS. For drug treatment, cells were maintained in MEM supplemented with 5.5% FBS and 20 mM HEPES. The use of human fibroblasts was approved by an Institutional Review Board at Weill Cornell Medical College for the research performed.

U2OS cells stably expressing of SRA

Human osteosarcoma U2OS (HTB-96TM) cells from ATCC (Manassas, VA) were transfected with murine SRA-II cDNA [kind gift from Dr. Monty Krieger (Massachusetts Institute of Technology, Boston, MA)]. Briefly, the 1.0 kb coding region of murine scavenger receptor type II was cut from a larger 4.0 kb plasmid encoding the coding region and the 3' untranslated region (UTR) in a pcDNA3.1 expression vector (41). The coding sequence was amplified by using PCR and inserted into a neomycin-resistant pcDNA 3.1 TOPO plasmid by using pcDNA 3.1 Directional TOPO Expression kit (Invitrogen), according to the manufacturer's instructions. The insertion of SRA-II in the pcDNA3.1 TOPO

plasmid was confirmed by band size of full-length plasmid and also after digestion with appropriate restriction enzymes using gel electrophoresis. The pcDNA 3.1 TOPO plasmid encoding SRA-II was purified by using the Qiagen DNA purification kit and transfected in U2OS cells by using Lipofectamine (Invitrogen) as a transfection reagent. U2OS cells expressing murine SRA-II were grown in McCoy's 5A medium supplemented with 10% FBS, 1% P/S, and selection antibiotic G418 (1 mg/ml) in a humidified incubator with 5% CO₂ at 37°C for five passages. To select a population of U2OS cells expressing the SRA-II gene, cells were incubated with DiIC18 (3) labeled AcLDL and sorted by using flow cytometry cell sorting. Murine macrophage cells J774 were used as a positive control, and the pool of cells with equivalent DiI intensity, indicative of SRA-II expression, were collected. The cells were expanded, and stock cultures were frozen for future experiments.

Effect of HDACi treatment on human fibroblasts

The dose dependence of two HDACis (vorinostat and panobinostat) was determined after 48 h treatment of NPC1 fibroblasts from several patients carrying different mutations. The assay is based on the use of filipin, a fluorescent dye that binds to unesterified cholesterol. Human fibroblasts were seeded in 384-well plates at 450 cells/well in growth medium on day one. Four cell lines were seeded in different wells of a plate, and GM03123 fibroblasts were used as a control in each plate. After overnight incubation, 2× concentrated compounds were added at six different doses, such that the final concentration ranged from 40 nM to 10 μM for vorinostat and 5 nM to 1 μM for panobinostat diluted in growth medium supplemented with 20 mM HEPES buffer and 5.5% FBS. DMSO was used as a control in each plate for each concentration and for each cell line. After 48 h, the plate was washed with PBS three times, fixed with 1.5% PFA, and stained with 50 μg/ml filipin and nuclear stain Draq5. Measurements were made from four wells for each condition in each experiment, and the experiment was repeated three times. Images were acquired on an ImageXpress^{Micro} automatic fluorescence microscope, at four sites per well and analyzed to obtain the LSO compartment ratio, which is a measure of filipin labeling of stored cholesterol (42). A high LSO ratio is associated with high levels of cholesterol in LE/Ly. Removal of this cholesterol leads to a reduction in the LSO ratio. The LSO compartment ratio for each concentration was normalized to corresponding DMSO treated control.

Persistence of vorinostat effects

NPC1 human fibroblasts GM03123 and GM18453 were seeded in four different 384 well plates at 450 cells/well in growth medium on day one. After overnight incubation, compounds diluted in growth medium supplemented with 20 mM HEPES buffer and 5.5% FBS were added in three of the four plates to achieve the desired final concentrations. DMSO was used as a control in each plate for each concentration. After 3 days, vorinostat-supplemented medium was aspirated from each plate and replaced with normal growth medium, and the cells were incubated for additional 0, 1, 2 or 3 days. At the end of each time point cells were stained with filipin, and the LSO ratio was determined. The experiment was performed twice independently. The LSO ratio for each concentration was normalized to a corresponding DMSO-treated value.

Stable silencing of NPC1

A line of NPC1-deficient stable U2OS-SRA cells was generated by silencing the endogenous NPC1 expression with 3'-UTR shNPC1 lentivirus. A Mission shRNA clone was purchased from

TABLE 1. List of mutations in NPC1 patient fibroblasts

GM03123	Heterozygous I1061T/ P237S
GM18453	Homozygous I1061T
NPC1-2	V1165M/ 3741-44 del ACTC
NPC1-5	I1061T/ R1186G
NPC1-16	P887L/ 3741-44 del ACTC
NPC1-17	I1061T, 10 bp deletion in exon 19 at codon 962 = fs(exon19)
NPC1-19	1920delG/ IVS9-1009G>A
NPC1-22	R978C, IVS21-2 A>G
NPC1-25	N701K/ C2979 dupA
NPC1-31	G46V/ L491P

Sigma-Aldrich against 3' UTR (TRCN000000542) of human NPC1 (pLKO-shNPC1) for knockdown of NPC1 expression. Stable clones of NPC1-deficient cells were selected with 5 µg/ml puromycin for 3 wk. Stable U2OS-SRA-shNPC1 cells were cultured in McCoy's 5A medium supplemented with 10% FBS, 50 units/ml penicillin, 50 µg/ml streptomycin, 5 µg/ml puromycin, and 1 mg/ml G418.

NPC1 expression vector

cDNA encoding human ΔU3hNPC1-WT construct was kindly provided by Dan Ory (Washington University, St Louis, MO). The NPC1 gene was subcloned into bicistronic retroviral plasmid, pMIEG3, by using EcoRI and NotI restriction enzyme sites. pMIEG3 vector was generated from pMSCVneo vector (Clontech) in which the murine phosphoglycerate kinase promoter and the Neomycin resistance (Neo^r) genes were replaced by internal ribosome entry site) and enhanced green fluorescent protein (eGFP) genes. The coexpression of eGFP with the NPC1 gene enables detection of cells expressing the human NPC1 protein by fluorescence microscopy. The WT construct used in this study has four variants as compared with a standard reference NPC1 sequence (37). These are: 387 T>C (Y129Y), 1,415 T>C (L472P), 1,925 T>C M642T, and 2,587 T>C (S863P). We found that these variants were also present in the human ΔU3hNPC1-WT construct, which has been used as a WT construct in previous publications (43). The ΔU3hNPC1-WT was derived from pSV-SPORT/NPC1, which has also been used as a WT in several previous studies (2, 44–46). Because the sequence differs from the reference NPC1 sequence, we will refer to these as WT variant (WT-V). By using WT-V pMIEG3-hNPC1 plasmid as a template, human NPC1 mutants were generated with Quick-Change XL Site-directed Mutagenesis Kit (Stratagene, La Jolla, CA). The pMIEG3 plasmid harbors an ampicillin resistance gene as a selection marker. These plasmids were transiently expressed in U2OS-SRA-shNPC1 cells. It should be noted that all of the mutant constructs contained the same variants as WT-V.

Reverse transfection, drug treatment, and cholesterol loading of U2OS-SRA-shNPC1 cells

By using the Effectene Transfection Reagent Kit, an expression vector containing one of the NPC1 mutants (0.4 µg DNA) was mixed with 3.2 µl enhancer in 100 µl of DNA-condensation buffer (EC) buffer for 5 min. They were then mixed with 4 µl Effectene in 100 µl EC buffer, and 5 µl of this mixture was added to each well of 384-well plates by using a Perkin Elmer Mini-JANUS liquid dispenser (PerkinElmer, Waltham, MA). The plates were centrifuged at 16 g for 10 min. U2OS-SRA-shNPC1 cells were prepared at 1.67×10^5 cells/ml in McCoy's 5A medium supplemented with 5% FBS, 1% P/S (medium A), and 5,000 cells (30 µl of U2OS-SRA-shNPC1 cells in medium A) were plated in each well of 384-well plates by using a Titertek Multidrop 384 model 832 liquid dispenser (Thermo Fisher Scientific Inc., Waltham, MA). Cells were grown with 30 µl medium A in a humidified incubator with 5% CO₂ at 37°C for 24 h. After 24 h, cells were treated with vorinostat (10 µM from a 5 mM stock in DMSO) or panobinostat (50 nM from a 5 mM DMSO stock) for 48 h. Control cells were treated with equivalent volumes of DMSO. The drugs in DMSO were diluted in medium A. To obtain final concentration of 10 µM for vorinostat treatment, 30 µl of the premixed 20 µM vorinostat in medium A was dispensed to each well by using a Thermo Multi-Drop liquid dispenser. To obtain final concentration of 50 nM for panobinostat treatment, 30 µl of the premixed 100 nM panobinostat in medium A was added into each well of the plates containing cells. After 48 h of treatment, cells were fixed with 1.5% PFA in PBS and stained with 50 µg/ml filipin in PBS (42). In order to load cells

with cholesterol, cells were treated with 50 µg/ml AcLDL in medium A for 2 h before fixation. All reagent additions, buffer changes, and labeling with filipin were carried out robotically by using a Thermo Multi-Drop liquid dispenser and a Bio-Tek Elx405 plate washer (Bio-Tek Instruments, Inc., Winooski, VT).

Fluorescence microscopy

An automated ImageXpress^{Micro} imaging system from Molecular Devices equipped with a 300 W Xenon-arc lamp from PerkinElmer, a Nikon 10× Plan Fluor 0.3 numerical aperture (NA) objective (Nikon, Tokyo, Japan), and a Photometrics CoolSnapHQ camera (1,392 × 1,040 pixels) from Roper Scientific was used to acquire images. Filipin images were acquired by using 377/50 nm excitation and 447/60 nm emission filters with a 415 dichroic long-pass (DCLP) filter. GFP images were acquired by using 472/30 nm excitation and 520/35 nm emission filters with a 669 DCLP filter. Filter sets assembled in Nikon filter cubes were obtained from Semrock.

NPC1 lifetime measurements

WT GM05659 and NPC1^{I1061T} mutant GM18453 skin fibroblasts were plated in 6-well plates at 50,000 cells per well. On day two, cells were treated with DMSO or vorinostat for 48 h in growth medium supplemented with 5.5% FBS. After 48 h, cells were switched to cysteine/methionine-free medium supplemented with 2% dialyzed FBS for 1 h, followed by a 1 h incubation with ³⁵S Cys/Met (150 µCi). In each experiment, two wells were used for competition control, to which 10× excess cysteine and methionine as compared with that in normal medium were added. The cells were subsequently washed twice with HBSS and chased in regular growth medium for times between 0 and 32 h. Cell lysates were prepared at each time point, after washing cells twice with HBSS and lysing in 500 µl nondenaturing lysis buffer (1% Triton X-100, 50 mM Tris-Cl, pH 7.4, 300 mM NaCl, 5 mM EDTA, 0.02% sodium azide, 10 mM iodoacetamide, 1 mM PMSF, and 2 µg/ml leupeptin). Separately, antibody-conjugated beads were prepared by combining 50% protein A-Sepharose bead slurry in ice-cold PBS and polyclonal rabbit antibody to NPC1 (6 µg/ml) and incubating the suspension at 4°C for 16 h. Beads were washed three times with nondenaturing lysis buffer and resuspended in 500 µl nondenaturing lysis buffer supplemented with 0.1% BSA. The entire cell lysate from each well was incubated with 30 µl of NPC1 antibody conjugated Protein A Sepharose beads in 500 µl in nondenaturing buffer for 2 h at 4°C while mixing on tube rotator. Beads were centrifuged and washed three times with ice-cold wash buffer (0.1% w/v triton X-100, 50 mM Tris-Cl, pH 7.4, 300 mM NaCl, 5 mM EDTA, 0.2% sodium azide). Beads were finally resuspended in 50 µl of 4× Laemmli SDS buffer and centrifuged. A total of 40 µl of each supernatant was analyzed by electrophoresis on 4–12% Bis-Tris gels (Nupage NP0321, Life Technologies, Grand Island, NY), followed by drying. Dried gels were exposed to a phosphor imager screen (Amersham Biosciences, Piscataway, NJ) overnight. The screen was scanned by using a Typhoon Trio PhosphorImager (GE Healthcare, Piscataway, NJ), and the images were saved as .tiff files. The integrated intensity of the bands at the molecular weight corresponding to NPC1 protein was measured by using Metamorph image analysis software. Within each condition, the intensities of bands corresponding to NPC1 protein were first corrected for background by subtracting the intensity at the same position in the competition control lane. Background-corrected values at each time were normalized to the value with no chase.

Western blot. Western blot analysis was performed on WT and HDACi-treated human NPC1 mutant fibroblasts by using a primary

polyclonal anti-rabbit NPC1 antibody from Abcam (Cambridge, MA). Secondary antibodies were from Pierce (Rockford, IL).

Imaging and analysis

A method described previously (42) was used to quantify the cholesterol accumulation in lysosomal storage organelles. NPC1 mutant cells show a bright region of filipin labeling near the cell center, corresponding to the sterol-loaded LSOs. The 384-well plates containing cells were imaged for GFP and filipin by using a 10× 0.3 NA dry objective on an ImageXpress^{Micro} automatic fluorescence microscope. Each well was imaged at four sites. Images were analyzed by using MetaXpress image-analysis software. First, all images were corrected for slightly inhomogeneous illumination as described previously (42). A background intensity value was set as the fifth percentile intensity of each image, and this intensity value was subtracted from each pixel in the image. At the plating density used in this study, all fields maintain at least 5% of the imaged area cell-free. To identify the cells expressing GFP, a threshold value was chosen for each experiment and was applied to GFP images. Objects containing at least 540 pixels above threshold were selected as transfected cells.

For the GFP-expressing cells, we obtained an LSO ratio, which is the ratio of filipin fluorescence intensity in the brightly labeled center of the cells divided by the area of the cells. The LSO ratio is determined by using two thresholds that are applied to the filipin images. A low threshold is set to include all areas occupied by cells. The outlines of cells using the low threshold are similar to cell outlines in transmitted light images. A higher threshold is then set to identify regions brightly stained with filipin in cells. The thresholds were chosen for each experiment. The LSO ratio of transfected cells on a per image basis was determined by using the following equation: LSO ratio=(Total intensity above high thresholded filipin intensity in GFP positive cells)/(Number of pixels above low thresholded filipin intensity in GFP positive cells).

Each NPC1 mutant was transfected in 12 wells of a 384-plate. Six wells were treated with drug 10 μM vorinostat or 50 nM panobinostat, and the other six were treated with DMSO as solvent control. WT-V and I1061T NPC1 were used as controls in each plate. There were three parallel plates for each experiment, and three independent experiments for each set of NPC1 mutants. The LSO ratio values for each experiment were normalized to the corresponding value for DMSO-treated I1061T NPC1 transfected cells. Normalized LSO ratio values from three independent experiments were averaged. The LSO ratio value for each NPC1 mutant with each treatment condition was averaged per image from 216 images (four sites × six wells × three plates × three experiments). In 216 images, there were approximately 40–120 images with GFP-positive cells. On average, there were three GFP-positive cells per image, so 120–360 NPC1 expressing cells were averaged to get the LSO ratio value for each NPC1 mutant with each treatment condition. A SEM was calculated for each LSO ratio value. A *P* value comparing LSO ratio values in DMSO-treated and drug-treated cells was calculated by using the *t* test with two-tailed distribution and two-sample equal variance (homoscedastic) type using Microsoft Excel software.

NPC1 immunolocalization in NPC1^{I1061T} human fibroblasts and U2OS-SRA-shNPC1 cells expressing NPC1^{I1061T}

WT human fibroblasts (GM05659), NPC1^{I1061T/P237S} (GM03123), and NPC1^{I1061T} (GM18453) human fibroblasts were treated with 10 μM vorinostat or DMSO solvent control for 48 h. Cells were then incubated with 50 μg/ml Alexa 546-LDL in MEM growth medium supplemented with 5.5% FBS and 10 μM vorinostat or

DMSO solvent control for 4 h, rinsed with growth medium, and chased in MEM growth medium supplemented with 5.5% FBS for 30 min. Cells were washed three times with PBS and then fixed with 1.5% PFA in PBS. For immunostaining, cells were permeabilized with 0.5% saponin and 10% goat serum (GS) in PBS for 30 min. Cells were incubated with 0.8 μg/ml anti-NPC1 rabbit polyclonal primary antibody for 2 h in the presence of 0.05% saponin and 0.5% GS at room temperature, followed by Alexa 488-labeled goat anti-rabbit secondary antibody (1:1,000; Life Technologies) for 45 min at room temperature. Finally, cells were washed three times with PBS, and images were acquired by using a wide-field microscope with a 63× 1.32 NA oil immersion objective and standard FITC and *tetramethylrhodamine isothiocyanate* filters.

U2OS-SRA-shNPC1 cells were transfected with WT-V or NPC1^{I1061T}. As described above, our WT NPC1 construct has four variants as compared with the reference NPC1 sequence. Thus, we describe it here as WT-V. One day after transfection, cells were treated with 10 μM vorinostat, 50 nM panobinostat, or DMSO solvent control. After 48 h treatment, cells were fixed with 1.5% PFA and processed for immunofluorescence as described above, except that 180 ng/ml anti-NPC1 rat monoclonal antibody (produced in the W. E. Balch laboratory) and 1:500 anti-LAMP1 rabbit polyclonal antibody were used, followed by a 1:1,000 dilution of Cy5 goat anti-rat and 1:500 of Alexa Fluor 546 goat anti-rabbit as secondary antibodies. Fluorescence images were acquired with a Zeiss LSM 510 laser-scanning confocal microscope (Zeiss, Thornwood, NY) using a 63× 1.4 NA objective (axial resolution 1.0 μm).

RESULTS

Protein lifetime measurements

Treatment with vorinostat and other HDACi increases the expression of the NPC1^{I1061T} protein in human patient-derived fibroblasts (19). Using procedures described in detail in Materials and Methods, we measured the effect of treatment with vorinostat on the lifetime of newly synthesized NPC1 protein in fibroblasts with a homozygous NPC1^{I1061T} mutation. WT and two sets of GM18453 cells were plated in 6-well plates on day 1. On day 2, WT and one set of GM18453 cells were treated with DMSO, and another set of GM18453 cells was treated with vorinostat for 48 h. After 48 h, all cells were incubated in Cys/Met-free medium for 1 h, followed by pulse-labeling for 1 h with ³⁵S Cys/Met, followed by a chase in complete medium for various times ranging from 0 to 32 h. Lysates of cells were immunoprecipitated with anti-NPC1 specific antibody (supplemental Fig. S1), followed by gel electrophoresis and determination of radioactivity at the molecular mass of NPC1 (210 kDa). As described previously (26), a substantial fraction of the WT NPC1 is degraded rapidly, and the remainder has a half time of more than a day. **Figure 1A** shows representative bands corresponding to the radiolabeled NPC1 protein from one experiment. For quantification, the intensity of the bands was measured for each time and corrected for background by subtracting the intensities for competition control. Corrected intensities in each experiment were normalized to the corresponding initial value. As shown in Fig. 1B, nearly all of the NPC1^{I1061T} protein was degraded rapidly in untreated cells. When cells

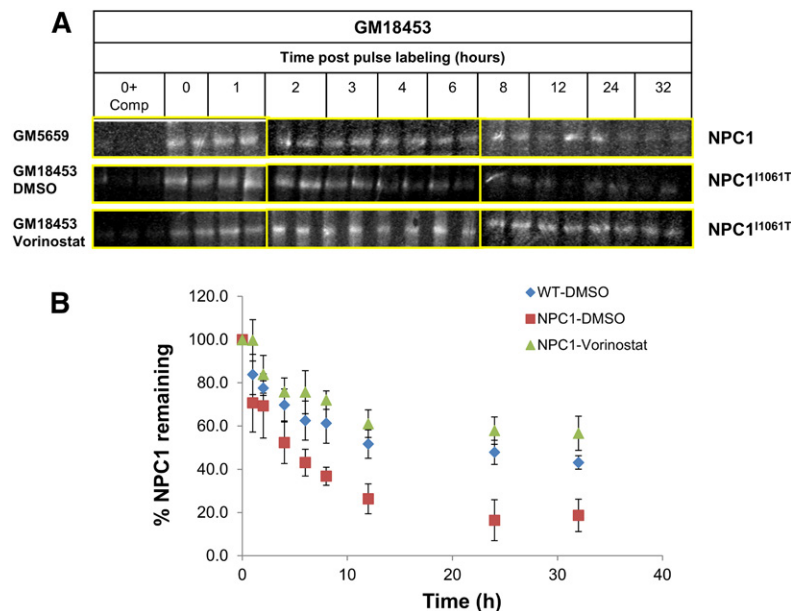


Fig. 1. NPC1 protein lifetime measurements. After 48 h treatment with 10 μ M vorinostat (or DMSO solvent control), GM05659 (WT) or GM18453 (NPC1^{I1061T}) fibroblasts were incubated for 1 h with Cys/Met-free culture medium supplemented with [³⁵S]Cys/Met, followed by a 0–32 h chase in normal culture medium. At the end of each chase time, cells were lysed, and cell lysates were immunoprecipitated (IP) with anti-NPC1 antibody. Protein antibody conjugates were resuspended in 50 μ l of 4 \times Laemmli SDS buffer, vortexed, and centrifuged, and 40 μ l was loaded on 4–12% Bis-Tris gels. Protein samples were separated by SDS-PAGE, and the densitometry values corresponding to radiolabeled NPC1 were measured. For each experiment, the values were normalized to the zero chase time value. A: Immunoprecipitated NPC1 bands as observed on the Phosphorimager screen. Left lanes for each condition show (0 h + competition control), which were used to correct for background noise. Duplicate samples for each time point in each experiment were set. Images shown are from one of five independent experiments. For each condition and cell type, samples were run on three separate gels as outlined by yellow bounding boxes. Images shown were from the gels run on the same day in parallel. B: Plot of the data are shown for solvent-treated GM05659 cells (blue diamonds), solvent-treated GM18453 cells (red squares), and vorinostat-treated GM18453 cells (green triangles). Each data point is representative of 10 values from 5 independent experiments \pm SEM.

with the NPC1^{I1061T} mutation were pretreated for 2 d with vorinostat (10 μ M), the protein degradation profile was remarkably similar to that seen for the WT protein. This indicates that treatment with an HDACi prevents the excessive degradation of the mutant protein.

HDACis lead to correct localization of mutant NPC1

To see whether the treatment with HDACi leads to correct targeting of the mutant protein, we examined the localization of mutant NPC1 protein in GM03123 (P237S and splice mutation, I1061T) (Fig. 2A) and in GM18453 (I1061T) (Fig. 2B) NPC1 mutant human fibroblasts. The cells were treated with 10 μ M vorinostat or solvent control DMSO for 48 h. The cells were then incubated with Alexa 546 LDL for 3.5 h, followed by a 0.5 h chase to deliver labeled LDL to LE/Ly (47–49). The cells were fixed, and NPC1 protein was detected by immunofluorescence (Fig. 2). Most of the mutant NPC1 protein did not colocalize with Alexa 546 LDL in LE/Ly in the DMSO-treated cells. After treatment with vorinostat, a large fraction of the mutant NPC1 protein localized in LE/Ly (yellow/orange color in overlays). This indicates that treatment with vorinostat leads to delivery of the mutant NPC1 to the organelles, in

which LDL is releasing cholesterol, which must be transported out of the organelles.

Testing the activity of vorinostat after drug withdrawal

If the effect of HDACi is to improve delivery of mutant NPC1 protein to LE/Ly, the effect should persist after removal of the drug because the NPC1 will remain in the organelles for more than a day. To test this, we performed Western blot analysis to determine the expression of NPC1 protein. GM18453 cells were plated in seven dishes. On the next day, DMSO was added in one dish, and 10 μ M vorinostat was added in six other dishes. Individual dishes of vorinostat-treated cells were lysed after 24, 48, and 72 h. After 72 h, the vorinostat-containing medium in the remaining three dishes was replaced by fresh growth medium. These dishes of cells were lysed after 24, 48, or 72 h. All seven lysates were run on SDS-PAGE, and Western blot analysis was performed. Shown in Fig. 3A are the bands corresponding to NPC1 protein and the loading control GAPDH for each time point. The levels of expression of the NPC1 protein remained elevated for 2–3 days after drug withdrawal.

To determine whether NPC1 is retained in LE/Ly after drug removal, cells were treated with DMSO or 10 μ M

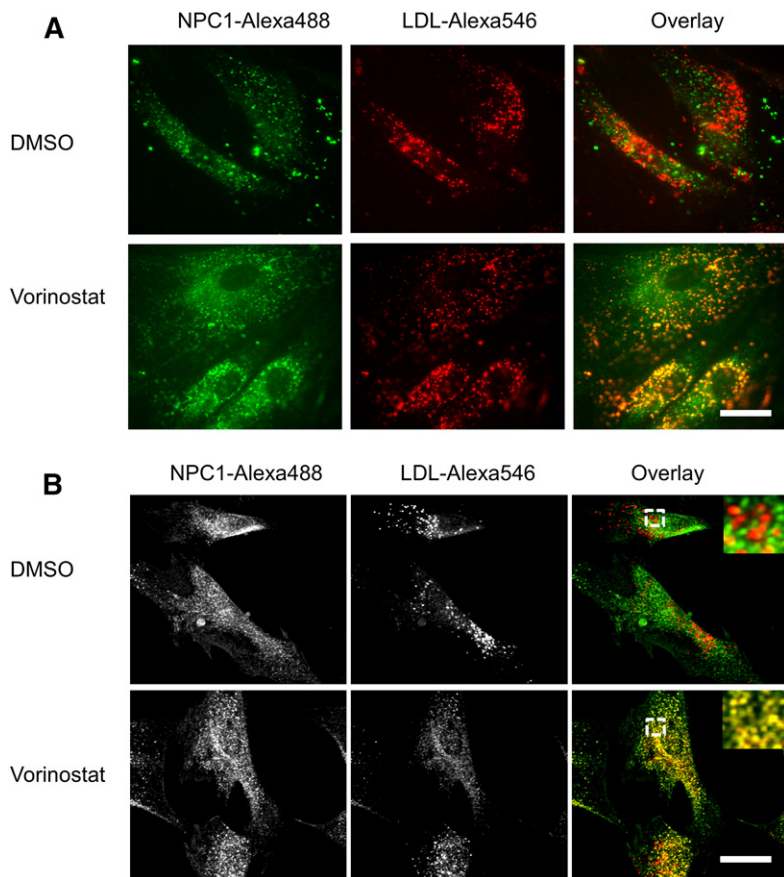


Fig. 2. Vorinostat rescues the localization of NPC1 in NPC1 mutant fibroblasts. GM03123 (A) or GM18453 (B) cells were plated in poly-D-lysine-coated cover-slip bottom dishes in MEM growth medium supplemented with 5.5% FBS. On day 2, cells were treated with DMSO or 10 μ M vorinostat and incubated for 48 h. For the last 4 h, cells were incubated with 50 μ g/ml Alexa 546-labeled LDL, followed by a 30 min chase in normal medium. Cells were fixed with 2% PFA, permeabilized, and immunostained for NPC1 with a rabbit anti-NPC1 antibody. Images were acquired on Zeiss LSM880 confocal microscope using a 63 \times objective. Images shown are maximum intensity projections. In (B), the region outlined in the overlay images is shown at higher magnification in the inset. Scale bars, 10 μ m.

vorinostat for 72 h, followed by 72 h in growth medium without vorinostat. Cells were fixed and permeabilized, followed by immunostaining for NPC1 and LAMP1 (supplemental Fig. S2). In DMSO-treated GM18453 fibroblasts, the NPC1 labeling was very weak, and the NPC1 was not in punctate organelles containing LAMP1. After vorinostat treatment for 72 h, the intensity of NPC1 labeling was

greatly enhanced, and the distribution colocalized well with punctate organelles containing LAMP1 (i.e., LE/Ly). This colocalization persisted for 72 h after withdrawal of vorinostat, although the NPC1 labeling became somewhat weaker.

To measure the cholesterol storage after drug withdrawal, NPC1 mutant human fibroblasts GM03123 (Fig. 3B)

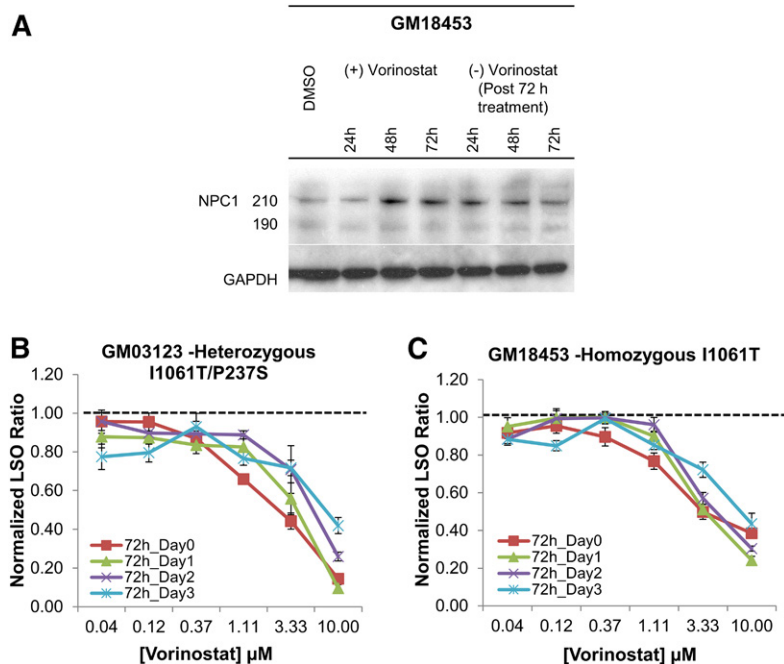


Fig. 3. Persistent effect of HDACi treatment in NPC1 mutant human fibroblasts. A: Immunoblot of cell lysates from GM18453 cells treated for 24, 48, or 72 h with 10 μ M vorinostat, followed by incubation for an additional 24, 48, or 72 h in the absence of vorinostat. Lysates were blotted with rabbit anti-NPC1 antibody and anti-GAPDH. Bands at 190 and 210 kDa represent glycosylated NPC1 protein. GM03123 (B) or GM 18453 (C) cells were treated with vorinostat at varying concentrations for 72 h. The cells were then incubated for an additional 0, 1, 2, or 3 days without vorinostat in normal growth medium. At the end of each time point, cells were stained with filipin, and the LSO value was measured to determine the relative amount of stored cholesterol. Data for each cell line are from two independent experiments, and each data point was obtained by using 48 images. Each data point is normalized to its corresponding DMSO-treated condition, so the value of 1 represents no effect. Error bars show SEM.

and GM18453 (Fig. 3C) were treated with vorinostat at varying concentrations for 72 h. The cells were rinsed and incubated for an additional 0, 1, 2, or 3 days in normal growth medium without vorinostat. At each time point, cells were fixed with PFA and stained with the cholesterol-binding dye filipin. We applied a quantitative image analysis method that has been described previously (19, 42) to measure cholesterol storage in the cells. The filipin-labeled cholesterol in LE/Ly is described by a parameter referred to as an “LSO value,” which measures the filipin fluorescence per cell in regions corresponding to the LSOs (see Materials and Methods). A high LSO ratio is associated with high levels of cholesterol in LE/Ly. The LSO values were determined relative to the corresponding DMSO control treatment, and the normalized value was plotted as a function of vorinostat concentration. Figure 3B, C shows that the activity of vorinostat to reduce stored cholesterol was retained for 2–3 days after withdrawal of drug. The persistence was observed at both 3.3 and 10 μM .

Treatment of several patient-derived human fibroblasts with vorinostat

We have shown previously that treatment with several HDACi corrects the cholesterol accumulation in homozygous and heterozygous I1061T mutant cell lines (19). To see whether vorinostat would also correct other NPC1 mutations, we tested its effect on cholesterol accumulation in eight lines of patient-derived fibroblasts (Table 1). All of the cell lines responded to vorinostat, but the dose response varied among the cell lines (Fig. 4A). Two cell lines (NPC1-17 and NPC1-25) had only partial reduction in cholesterol storage after 48 h of vorinostat treatment, whereas the NPC1-22 cells were nearly completely corrected by approximately 1 μM vorinostat. These results indicate that vorinostat treatment can correct the NPC1 phenotype in cell lines with several different compound heterozygous mutations. Similar results were obtained with panobinostat, and NPC1-25 was also only partially responsive to panobinostat as compared with the other cell lines tested (Fig. 4B). As observed previously (19), high concentrations of panobinostat lead to higher levels of cholesterol storage. This probably reflects the effects of HDACi treatment on expression of many genes (50).

Effect of HDACi in cells expressing NPC1 mutants

To test the effect of HDACi on individual NPC1 mutations, we established a cell line that lacked expression of endogenous NPC1 and expressed SRA to allow efficient uptake of lipoprotein-derived cholesterol. We stably transfected SRA into a human osteosarcoma cell line, U2OS cells, that has been used widely in drug-screening trials (51, 52). These U2OS-SRA cells were then stably transfected with a plasmid expressing shRNA targeting a nontranslated region of the NPC1 mRNA to silence the expression of endogenous NPC1. A library of disease-associated NPC1 mutants was created in a bicistronic vector also expressing GFP to identify the transfected cells. By using reverse transfection, different NPC1 mutants were transfected into individual wells of a 384-well plate. Half of the wells were treated

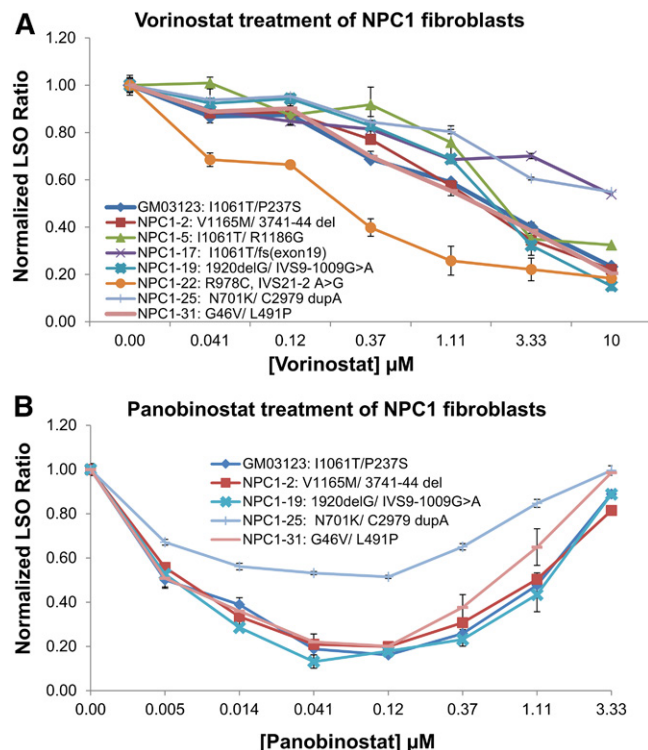


Fig. 4. Dose-dependent effect of vorinostat and panobinostat on multiple patient-derived NPC1 mutant cell lines. NPC1 mutant human fibroblasts were treated with vorinostat (A) or panobinostat (B) for 48 h, followed by fixation, staining with filipin, and imaging by using the ImageXpress^{Micro} automatic fluorescence microscope. DMSO was used as a solvent control. Images were analyzed to obtain the LSO value as a measure of cholesterol accumulation. Data were normalized to the corresponding DMSO-treated cells. Data for each cell line are averages of three independent experiments totaling 60 images (5 wells \times 4 sites \times 3 experiments). Error bars show SEM.

with an HDACi (in DMSO), whereas the other half were treated with the same amount of DMSO as a solvent control. The NPC1 sequence used in these experiments contained four variants as compared with an NPC1 reference sequence, and we describe this as an NPC-V sequence (see Materials and Methods for details). The NPC-V was also used as the basis for constructing the individual mutations that were being analyzed. Vectors expressing WT-V NPC1 and NPC1^{I1061T} were included in each plate as controls. A more complete description of the NPC-V variant and its use in previous studies will be published elsewhere.

Figure 5 illustrates the screening process. After transfection and drug treatment, cells were fixed and stained with filipin. Untransfected U2OS-SRA-shNPC1 cells incubated with 50 $\mu\text{g}/\text{ml}$ AcLDL for 2 h are brightly labeled with filipin (Fig. 5A), reflecting the high levels of unesterified cholesterol stored in the LSOs of these cells (19, 42, 53). Cells transfected with WT-V NPC1 (i.e., those expressing GFP) showed greatly reduced filipin labeling as compared with their untransfected neighbors (Fig. 5A). Cells transfected with NPC1^{I1061T} (expressing GFP) showed little, if any, decrease in filipin labeling as compared with their untransfected neighbors. However, treatment of these NPC1^{I1061T}-transfected cells with either vorinostat

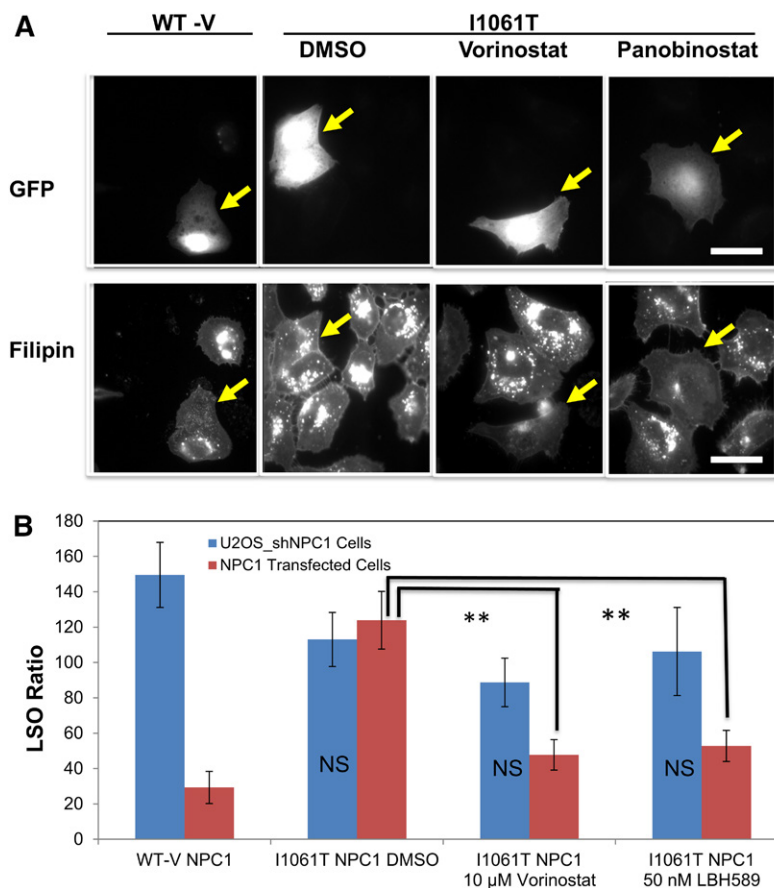


Fig. 5. Illustration of the screening system. **A:** Representative images of transfected cells. At 24 h after transfection with a bicistronic vector containing eGFP plus WT-V-NPC1 or NPC1^{I1061T}, U2OS-SRA-shNPC1 cells were treated with vorinostat (10 μ M), panobinostat (50 nM), or DMSO solvent control for 48 h. Cells were treated with 50 μ g/ml AcLDL for the final 2 h, fixed with PFA, and stained with filipin. Images were acquired on a Leica wide-field microscope using standard GFP and A4 filters. Transfection with WT NPC1 reduced the cholesterol accumulation, but transfection with NPC1^{I1061T} did not, unless they were treated with an HDACi. Scale bar 10 μ m. **B:** Quantification of filipin in transfected cells. Cholesterol accumulation in LSO of GFP-positive cells was measured based on filipin fluorescence, and the LSO values are shown. As described in Materials and Methods, images were obtained from 216 fields in three experiments for each condition. Between 40 and 120 of these images had GFP-labeled cells, and the LSO value was obtained for each of these images. In each experiment, the LSO values were normalized to the solvent-treated control. These normalized LSO values were used for statistical analysis. Error bars show SEM. ** $P < 0.01$.

(10 μ M) or panobinostat (50 nM) for 2 days greatly reduced the filipin labeling of transfected cells, with no discernible effect on the untransfected neighbors. This indicates that the NPC1^{I1061T} protein can effectively remove cholesterol from LSOs in cells treated with an effective dose of an HDACi. These results also show that treatment with an HDACi does not correct the cholesterol storage defect in cells lacking NPC1 expression.

To quantify the relative amount of cholesterol storage under various conditions, we measured the LSO values (19, 42). Figure 5B shows the quantitative analysis of the effects of transfecting U2OS-SRA-shNPC1 with WT-V NPC1 or NPC1^{I1061T}. Expression of the NPC1^{I1061T} mutant only caused a significant decrease in the LSO value in cells treated with an HDACi. No significant effect on the LSO value was seen in untransfected U2OS-SRA-shNPC1 cells treated with the HDACi.

As with the human patient fibroblasts (Fig. 2), treatment of U2OS-SRA-shNPC1 cells expressing NPC1^{I1061T} with an HDACi led to delivery of the mutant NPC1 to LE/Ly labeled with antibodies to the abundant lysosome-associated membrane protein, LAMP1 (54) (Fig. 6). When U2OS-SRA-shNPC1 cells were transfected with WT-V NPC1 (top row), there was good colocalization of the NPC1 (detected by immunofluorescence) with the LAMP1, indicating that a high fraction of the NPC1 protein was in LE/Ly. When cells were transfected with NPC1^{I1061T} (second row), there was little colocalization of NPC1 with LAMP1, indicating a

failure to deliver the mutant NPC1 to LE/Ly. However, if the cells transfected with NPC1^{I1061T} were treated with vorinostat (third row) or panobinostat (fourth row), there was significant colocalization of the mutant NPC1 with the LAMP1, as seen by the yellow/orange organelles in the overlays. An untransfected cell lacking GFP expression in the third row did not show labeling with the rat monoclonal NPC1 antibody, verifying the specificity of the antibody (32).

The full-length NPC1 protein has 13 transmembrane domains and three large luminal domains. These are clustered into six different groups (Figs. 7, 8). As described in Materials and Methods, 60 different NPC1 mutants that have been found in patients were transiently transfected into U2OS-SRA-shNPC1 cells. Using the assay for filipin labeling, we tested the effect of vorinostat (10 μ M) and panobinostat (50 nM) on cells expressing these 60 different NPC1 mutations (Fig. 7 and supplemental Fig. S3). With vorinostat or panobinostat treatment, 52 of the 60 mutants showed a reduction of the LSO value, with $P < 0.05$ (blue bars). (Mutants that showed no change or reduction of LSO value with $P > 0.05$ are plotted in red/pink.) As expected, the LSO values for WT-V-transfected cells were not reduced significantly after HDACi treatment, as shown by the first set of red bars in each plot.

The results are summarized in Fig. 8. Mutants that showed a statistically significant ($P < 0.05$) response to vorinostat are listed in black, and nonresponsive mutants

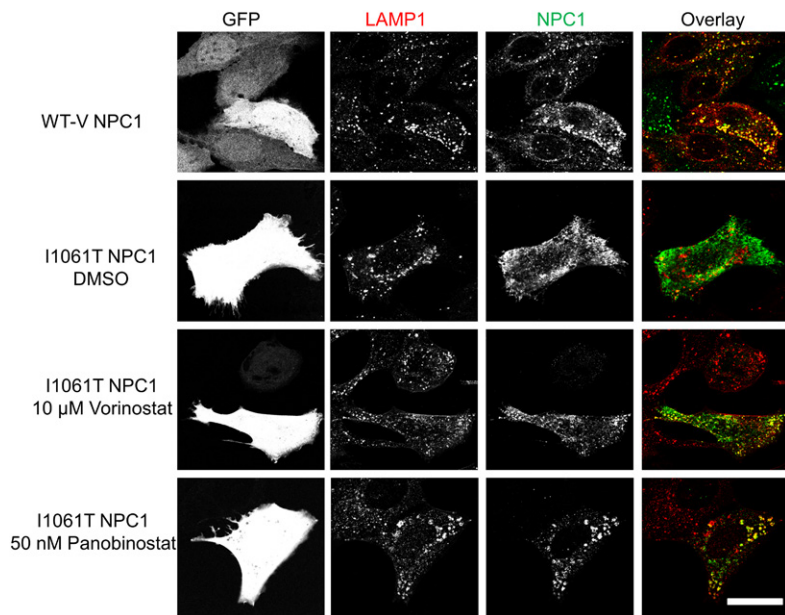


Fig. 6. Vorinostat and panobinostat rescue localization of NPC1^{I1061T} in U2OS-SRA-shNPC1 cells. WT-V NPC1 or NPC1^{I1061T} was expressed in U2OS-SRA-shNPC1 cells by using a bicistronic vector also encoding eGFP. Starting 1 day later, wells transfected with NPC1^{I1061T} were treated with 10 μ M vorinostat, 50 nM panobinostat, or DMSO solvent control for 48 h. GFP serves as a marker of transfected cells. NPC1 protein was detected by immunofluorescence using anti-NPC1 rat monoclonal primary antibody and Cy5 goat anti-rat secondary antibody. Lysosomes were identified by using anti-LAMP1 rabbit polyclonal antibody and Alexa Fluor 546 goat anti-rabbit secondary antibody. The colocalizations of NPC1 protein and LE/Ly are shown in yellow. Scale bar, 10 μ m.

are listed in red. More than 85% of the mutations showed a statistically significant response to either of the HDACi treatments. Some of the mutants that were not corrected to a statistically significant level had low starting cholesterol, which made it more difficult to demonstrate an effect. Expression of these mutants may have had some corrective effect, even before HDACi treatment. In general, the data shown in Fig. 7 indicate that there is not a strong correlation between the LSO value before treatment and the correction seen after HDACi treatment. After HDACi treatment, many of the mutants that showed high cholesterol storage before treatment were corrected to nearly the level in WT-V transfectants.

A full listing of the mutants and the statistical significance of their responses is provided in supplemental Table S1. To see whether correction depended on the severity of the initial cholesterol accumulation, we compared the LSO values of DMSO-treated and vorinostat- or panobinostat-treated cells. It can be seen that most of the mutations with the highest initial cholesterol storage were corrected.

DISCUSSION

NPC disease is a devastating inherited disorder with no FDA-approved treatment. More than 300 disease-causing mutations have been found in NPC1 (10, 37), and most of these are missense mutations in this large membrane protein. As part of a screen for compounds that would correct the cholesterol storage defect in patient-derived fibroblasts, we found that several HDACi compounds were included among the hits (19). The pharmacological profile of the effective inhibitors suggested that HDACs 1, 2, or 3 were the most relevant targets (19, 20). Although increased expression of the NPC1^{I1061T} protein was observed after treatment with HDACi, the mechanism of correction and the applicability to a variety of mutations were not determined.

It has been shown previously that nearly half of the WT NPC1 protein is degraded by an ERAD pathway, and essentially all of the newly synthesized NPC1^{I1061T} protein is degraded by ERAD (26). In this study, we found that treatment of cells with vorinostat causes the stability of the NPC1^{I1061T} protein to be indistinguishable from the WT protein. The longer-lived fraction of both WT and HDACi-treated NPC1^{I1061T} were degraded with a half-time of more than 1 day. We also observed that the NPC1^{I1061T} protein was correctly delivered to LE/Ly that contain endocytosed LDL, so after exit from the endoplasmic reticulum (ER), a significant amount of the mutant protein was trafficked to the correct organelle. The effect of HDACi treatment on cholesterol storage in LSOs persisted for 2–3 days after withdrawal of the drug, which is consistent with the long lifetime of the NPC1^{I1061T} protein after it has passed the ER quality-control system. The long-term effect of the HDACi after removal from the medium may be useful in designing clinical protocols because the drug may only have to be administered intermittently.

HDACi treatments corrects the cholesterol storage in cells expressing a large majority of NPC1 mutations

In order to test the effect of HDACi treatment on a large number of mutants, we used a reverse transfection strategy that could be used for screening in multiwell plates (55). The U2OS-SRA-shNPC1 cells were developed for this purpose. The stable expression of SRA was valuable because it allowed us to deliver a large amount of cholesterol to the cells via AcLDL, which binds to SRA and is internalized by receptor-mediated endocytosis (56). Cells with defects in the NPC1 protein were unable to clear this bolus of cholesterol from the LE/Ly.

It was shown previously that very high levels of overexpression of the NPC1^{I1061T} protein can correct the cholesterol storage defect in cells, presumably because a small fraction of the protein gets into the LE/Ly (26). We did not measure expression levels of the various mutants, but

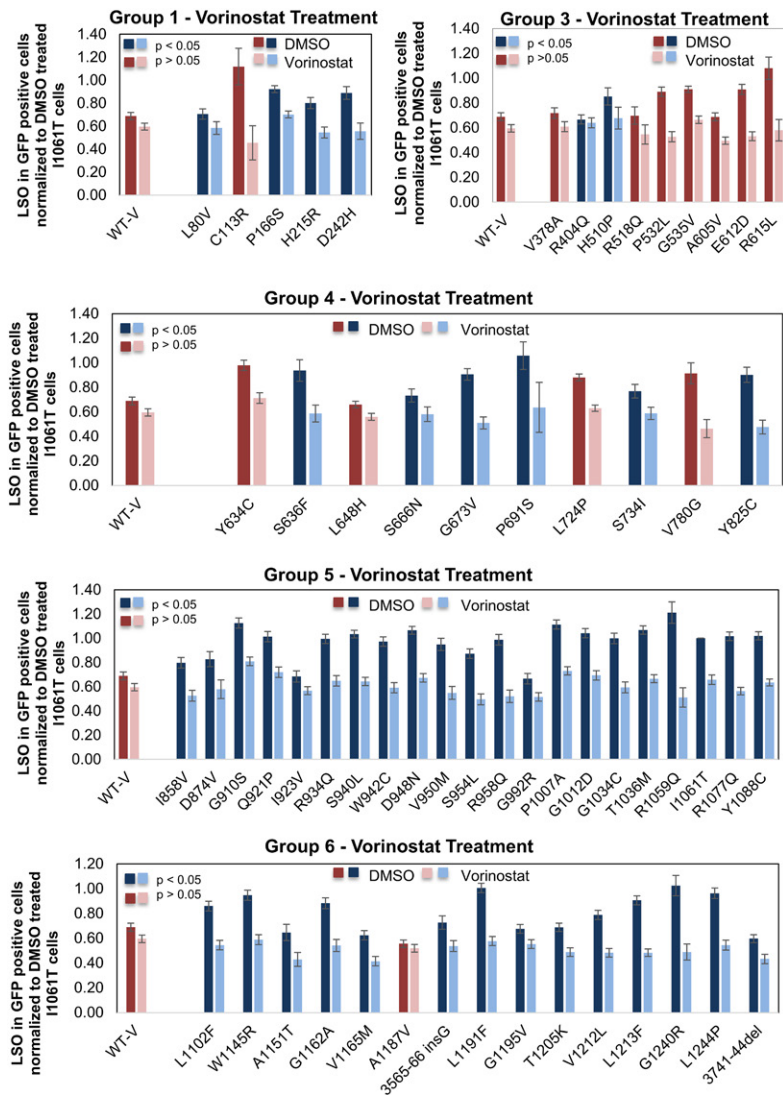


Fig. 7. Quantification of effects of vorinostat on cholesterol accumulation in NPC1 mutants. The effect of 10 μ M vorinostat was tested on 60 different NPC1 mutations from five segments of the NPC1 protein as illustrated in Fig. 8. DMSO was used as a solvent control. Filipin fluorescence images of the transfected cells were analyzed to obtain an LSO value as explained in Materials and Methods. Data represent averages \pm SEM from 15–25 images. Each image includes approximately one to five transfected cells. Dark blue bars (DMSO-treated) and light blue bars (vorinostat-treated) for each group represent mutants that showed reduction in LSO values with $P < 0.05$, and dark red bars (DMSO-treated) and pink bars (vorinostat-treated) represent mutants that showed no significant reduction in LSO value. Statistical significance was measured by t test with two-tailed distribution and two-sample equal variance (homoscedastic) type using Microsoft Excel software.

we did find that most mutants did not correct the cholesterol storage in the absence of drug treatment. We observed that more than 85% of the NPC1 mutants could be corrected for their cholesterol accumulation by treatment with either vorinostat or panobinostat. This indicates that

more than 90% of patients would be expected to have at least one allele that is susceptible to HDACi treatment. Mechanistically, this suggests that the large majority of NPC1 missense mutations can be functional if they are delivered to the correct organelles.

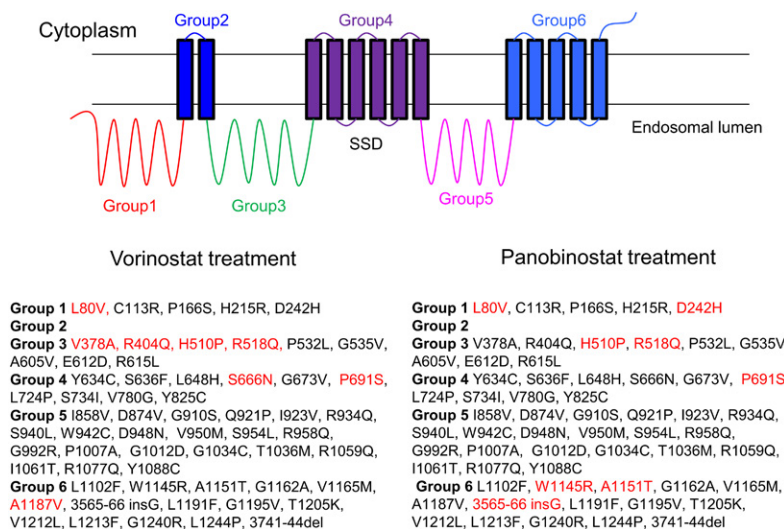


Fig. 8. List of NPC1 mutants tested with vorinostat and panobinostat. A total of 60 NPC1 mutants were treated with vorinostat (10 μ M) or panobinostat (50 nM) as described in Fig. 7. The mutants are separated into six groups by their locations in the NPC1 protein structure. Mutants that showed a statistically significant ($P < 0.05$) response to vorinostat are listed in black, and nonresponsive mutants ($P > 0.05$) are in red.

The analysis of the mutants that can and cannot be corrected provides some insight into the requirements for a functional NPC1 protein. One caveat is that these assays were carried out in a high-throughput screening system, and they have not been individually verified in detail. However, analysis of the data provides some measures of quality control. First, it should be noted that there is a good general correspondence between the mutations that were affected by vorinostat and those affected by panobinostat. Some of the mutants that were listed as corrected by one drug, but not the other, were only statistically significant at $P < 0.05$ (supplemental Table S1), suggesting that these might have been only partially corrected by one or both HDACis.

Mutations resistant to HDACi treatment


The lack of effect of both vorinostat and panobinostat is consistent with the lack of an effect of HDACi treatment on cells lacking NPC1 expression. One of the noncorrected mutations (L80V) is in the N-terminal domain, which is responsible for cholesterol binding. The leucine at position 80 is close to the cholesterol-binding pocket (4). NPC2 binds to the first luminal loop (group 3 in Fig. 8) of NPC1, and it has been shown that mutations R404Q and R518Q interfere with this binding (57). Neither of these mutations was corrected by vorinostat, and R518Q is not corrected by panobinostat. It has been shown that NPC1^{R518Q} goes to punctate organelles in a distribution consistent with LE/Ly without drug treatment (57). The P691S mutation is in the sterol-sensing domain of NPC1 (35). It has been shown that this mutation is ineffective in promoting cholesterol transport, even though it is delivered correctly to LE/Ly (58). It is noteworthy that all of the mutations in group 5 can be rescued by both vorinostat and panobinostat. Apparently, this segment of NPC1 can tolerate many mutations without losing the ability to export cholesterol from LE/Ly.

Mechanism of correction by HDACi

The mechanism by which HDACi treatment rescues the function of mutant NPC1 proteins will require further mechanistic studies. One possibility is that HDACi treatment alters the proteostatic environment (30–32). This would allow more of the mutant protein to escape ERAD, as is illustrated for NPC1^{I1061T} in Fig. 1. It has been reported that HDACi treatment can increase expression of some protein chaperonins (59) or directly modulate the activity of chaperones by altering their acetylation status (60). As discussed in the Introduction, treatments that would be expected to enhance NPC1 folding in the ER, such as chemical chaperones or treatments that alter ER chaperone activity, have been shown to correct the storage defect in some NPC1 mutant cell lines (27–29).

An indirect mechanism for overcoming the cholesterol accumulation caused by mutations in NPC1 is consistent with findings that patients with identical mutations can have different times to initial onset and disease severity (10). This suggests that other factors in the genetic background can alter the degree of loss of function. It is not

known whether this is related to higher levels of correct targeting of mutant NPC1 protein in the tissues of less affected individuals.

Our data suggest that the vast majority of NPC1 patients carry mutations that could be corrected by HDACi treatment. vorinostat and panobinostat are FDA-approved drugs for treatment of some cancers, and HDACi have been used in clinical trials for many other diseases (20). Vorinostat is generally well tolerated as a cancer therapeutic agent (61). Several other HDACis have been in large-scale clinical trials. Because the most important pathologies of NPC disease are related to neuronal cell dysfunction and death (10), penetration of an HDACi into the brain will be essential for effective treatment. Some HDACis have excellent penetration into the brain and have been used in animal and human studies for treatment of neurological diseases (20). The results described here support the investigation of HDACi as single or combination therapies (34) for NPC1 disease. 

The authors thank Dr. Forbes D. Porter (National Institute of Child Health and Human Development, Bethesda, MD) for supplying several NPC patient fibroblast cell lines; Dr. Dan Ory (Washington University, St. Louis, MO) for providing NPC1 cDNA; and Dr. Paul Helquist (University of Notre Dame, South Bend, IN) for supplying vorinostat and panobinostat.

REFERENCES

1. Naureckiene, S., D. E. Sleat, H. Lackland, A. Fensom, M. T. Vanier, R. Wattiaux, M. Jadot, and P. Lobel. 2000. Identification of HE1 as the second gene of Niemann-Pick C disease. *Science*. **290**: 2298–2301.
2. Watari, H., E. J. Blanchette-Mackie, N. K. Dwyer, J. M. Glick, S. Patel, E. B. Neufeld, R. O. Brady, P. G. Pentchev, and J. F. Strauss 3rd. 1999. Niemann-Pick C1 protein: obligatory roles for N-terminal domains and lysosomal targeting in cholesterol mobilization. *Proc. Natl. Acad. Sci. USA*. **96**: 805–810.
3. Infante, R. E., M. L. Wang, A. Radhakrishnan, H. J. Kwon, M. S. Brown, and J. L. Goldstein. 2008. NPC2 facilitates bidirectional transfer of cholesterol between NPC1 and lipid bilayers, a step in cholesterol egress from lysosomes. *Proc. Natl. Acad. Sci. USA*. **105**: 15287–15292.
4. Kwon, H. J., L. Abi-Mosleh, M. L. Wang, J. Deisenhofer, J. L. Goldstein, M. S. Brown, and R. E. Infante. 2009. Structure of N-terminal domain of NPC1 reveals distinct subdomains for binding and transfer of cholesterol. *Cell*. **137**: 1213–1224.
5. Li, X., J. Wang, E. Coutavas, H. Shi, Q. Hao, and G. Blobel. 2016. Structure of human Niemann-Pick C1 protein. *Proc. Natl. Acad. Sci. USA*. **113**: 8212–8217.
6. Gong, X., H. Qian, X. Zhou, J. Wu, T. Wan, P. Cao, W. Huang, X. Zhao, X. Wang, P. Wang, et al. 2016. Structural insights into the Niemann-Pick C1 (NPC1)-mediated cholesterol transfer and Ebola infection. *Cell*. **165**: 1467–1478.
7. Li, X., P. Saha, J. Li, G. Blobel, and S. R. Pfeffer. 2016. Clues to the mechanism of cholesterol transfer from the structure of NPC1 middle luminal domain bound to NPC2. *Proc Natl Acad Sci USA* **113**: 10079–10084.
8. Pipalia, N. H., M. Hao, S. Mukherjee, and F. R. Maxfield. 2007. Sterol, protein and lipid trafficking in Chinese hamster ovary cells with Niemann-Pick type C1 defect. *Traffic*. **8**: 130–141.
9. Choudhury, A., D. K. Sharma, D. L. Marks, and R. E. Pagano. 2004. Elevated endosomal cholesterol levels in Niemann-Pick cells inhibit rab4 and perturb membrane recycling. *Mol. Biol. Cell*. **15**: 4500–4511.
10. Vanier, M. T. 2010. Niemann-Pick disease type C. *Orphanet J. Rare Dis*. **5**: 16.

11. Patterson, M., M. Vanier, K. Suzuki, J. Morris, E. Carstea, E. Neufeld, E. Blanchette-Mackie, and P. Pentchev. 2001. Niemann-Pick Disease Type C: A lipid Trafficking Disorder. McGraw-Hill, New York.
12. Platt, F. M., G. R. Neises, R. A. Dwek, and T. D. Butters. 1994. N-Butyldeoxynojirimycin is a novel inhibitor of glycolipid biosynthesis. *J. Biol. Chem.* **269**: 8362–8365.
13. Patterson, M. C., D. Vecchio, E. Jacklin, L. Abel, H. Chadha-Boreham, C. Luzy, R. Giorgino, and J. E. Wraith. 2010. Long-term miglustat therapy in children with Niemann-Pick Disease type C. *J. Child Neurol.* **25**: 300–305.
14. Patterson, M. C., D. Vecchio, H. Prady, L. Abel, and J. E. Wraith. 2007. Miglustat for treatment of Niemann-Pick C disease: a randomised controlled study. *Lancet Neurol.* **6**: 765–772.
15. Davidson, C. D., N. F. Ali, M. C. Micsenyi, G. Stepney, S. Renault, K. Dobrenis, D. S. Ory, M. T. Vanier, and S. U. Walkley. 2009. Chronic cyclodextrin treatment of murine Niemann-Pick C disease ameliorates neuronal cholesterol and glycosphingolipid storage and disease progression. *PLoS One.* **4**: e6951.
16. Liu, B., S. D. Turley, D. K. Burns, A. M. Miller, J. J. Repa, and J. M. Dietschy. 2009. Reversal of defective lysosomal transport in NPC disease ameliorates liver dysfunction and neurodegeneration in the npc1^{-/-} mouse. *Proc. Natl. Acad. Sci. USA.* **106**: 2377–2382.
17. Vite, C. H., J. H. Bagel, G. P. Swain, M. Prociuk, T. U. Sikora, V. M. Stein, P. O'Donnell, T. Ruane, S. Ward, A. Crooks, et al. 2015. Intracisternal cyclodextrin prevents cerebellar dysfunction and Purkinje cell death in feline Niemann-Pick type C1 disease. *Sci. Transl. Med.* **7**: 276ra26.
18. Maarup, T. J., A. H. Chen, F. D. Porter, N. Y. Farhat, D. S. Ory, R. Sidhu, X. Jiang, and P. I. Dickson. 2015. Intrathecal 2-hydroxypropyl-beta-cyclodextrin in a single patient with Niemann-Pick C1. *Mol. Genet. Metab.* **116**: 75–79.
19. Pipalia, N. H., C. C. Cosner, A. Huang, A. Chatterjee, P. Bourbon, N. Farley, P. Helquist, O. Wiest, and F. R. Maxfield. 2011. Histone deacetylase inhibitor treatment dramatically reduces cholesterol accumulation in Niemann-Pick type C1 mutant human fibroblasts. *Proc. Natl. Acad. Sci. USA.* **108**: 5620–5625.
20. Helquist, P., F. R. Maxfield, N. L. Wiech, and O. Wiest. 2013. Treatment of Niemann-pick type C disease by histone deacetylase inhibitors. *Neurotherapeutics.* **10**: 688–697.
21. Munkacsy, A. B., F. W. Chen, M. A. Brinkman, K. Higaki, G. D. Gutierrez, J. Chaudhari, J. V. Layer, A. Tong, M. Bard, C. Boone, et al. 2011. An “exacerbate-reverse” strategy in yeast identifies histone deacetylase inhibition as a correction for cholesterol and sphingolipid transport defects in human Niemann-Pick type C disease. *J. Biol. Chem.* **286**: 23842–23851.
22. Rosenbaum, A. I., G. Zhang, J. D. Warren, and F. R. Maxfield. 2010. Endocytosis of beta-cyclodextrins is responsible for cholesterol reduction in Niemann-Pick type C mutant cells. *Proc. Natl. Acad. Sci. USA.* **107**: 5477–5482.
23. Palmieri, D., P. R. Lockman, F. C. Thomas, E. Hua, J. Herring, E. Hargrave, M. Johnson, N. Flores, Y. Qian, E. Vega-Valle, et al. 2009. Vorinostat inhibits brain metastatic colonization in a model of triple-negative breast cancer and induces DNA double-strand breaks. *Clin. Cancer Res.* **15**: 6148–6157.
24. Food and Drug Administration. 2014. Application no. 205353Orig1s000; Farydak (panobinostat) http://www.accessdata.fda.gov/drugsatfda_docs/nda/2015/205353Orig1s000PharmR.pdf
25. Schroeder, F. A., D. B. Chonde, M. M. Riley, C. K. Moseley, M. L. Granda, C. M. Wilson, F. F. Wagner, Y-L. Zhang, J. Gale, E. B. Holson, et al. 2013. FDG-PET imaging reveals local brain glucose utilization is altered by class I histone deacetylase inhibitors. *Neurosci. Lett.* **550**: 119–124.
26. Gelsthorpe, M. E., N. Baumann, E. Millard, S. E. Gale, S. J. Langmade, J. E. Schaffer, and D. S. Ory. 2008. Niemann-Pick type C1 I1061T mutant encodes a functional protein that is selected for endoplasmic reticulum-associated degradation due to protein misfolding. *J. Biol. Chem.* **283**: 8229–8236.
27. Yu, T., C. Chung, D. Shen, H. Xu, and A. P. Lieberman. 2012. Ryanodine receptor antagonists adapt NPC1 proteostasis to ameliorate lipid storage in Niemann-Pick type C disease fibroblasts. *Hum. Mol. Genet.* **21**: 3205–3214.
28. Ohgane, K., F. Karaki, K. Dodo, and Y. Hashimoto. 2013. Discovery of oxysterol-derived pharmacological chaperones for NPC1: implication for the existence of second sterol-binding site. *Chem. Biol.* **20**: 391–402.
29. Ebrahimi-Fakhari, D., L. Wahlster, F. Bartz, J. Werenbeck-Ueding, M. Praggastis, J. Zhang, B. Jogerst-Thomalla, S. Theiss, D. Grimm, D. S. Ory, et al. 2016. Reduction of TMEM97 increases NPC1 protein levels and restores cholesterol trafficking in Niemann-pick type C1 disease cells. *Hum. Mol. Genet.* **25**: 3588–3599.
30. Calamini, B., M. C. Silva, F. Madoux, D. M. Hutt, S. Khanna, M. A. Chalfant, S. A. Saldanha, P. Hodder, B. D. Tait, D. Garza, et al. 2011. Small-molecule proteostasis regulators for protein conformational diseases. *Nat. Chem. Biol.* **8**: 185–196.
31. Hutt, D. M., E. T. Powers, and W. E. Balch. 2009. The proteostasis boundary in misfolding diseases of membrane traffic. *FEBS Lett.* **583**: 2639–2646.
32. Rauniyar, N., K. Subramanian, M. Lavallée-Adam, S. Martínez-Bartolomé, W. E. Balch, and J. R. Yates. 2015. Quantitative proteomics of human fibroblasts with I1061T mutation in Niemann-Pick C1 (NPC1) protein provides insights into the disease pathogenesis. *Mol. Cell. Proteomics.* **14**: 1734–1749.
33. Praggastis, M., B. Tortelli, J. Zhang, H. Fujiwara, R. Sidhu, A. Chacko, Z. Chen, C. Chung, A. P. Lieberman, J. Sikora, et al. 2015. A murine Niemann-Pick C1 I1061T knock-in model recapitulates the pathological features of the most prevalent human disease allele. *J. Neurosci.* **35**: 8091–8106.
34. Alam, M. S., M. Getz, and K. Haldar. 2016. Chronic administration of an HDAC inhibitor treats both neurological and systemic Niemann-Pick type C disease in a mouse model. *Sci. Transl. Med.* **8**: 326ra23.
35. Davies, J. P., and Y. A. Ioannou. 2000. Topological analysis of Niemann-Pick C1 protein reveals that the membrane orientation of the putative sterol-sensing domain is identical to those of 3-hydroxy-3-methylglutaryl-CoA reductase and sterol regulatory element binding protein cleavage-activating protein. *J. Biol. Chem.* **275**: 24367–24374.
36. Millat, G., C. Marçais, M. A. Rafi, T. Yamamoto, J. A. Morris, P. G. Pentchev, K. Ohno, D. A. Wenger, and M. T. Vanier. 1999. Niemann-Pick C1 disease: the I1061T substitution is a frequent mutant allele in patients of Western European descent and correlates with a classic juvenile phenotype. *Am. J. Hum. Genet.* **65**: 1321–1329.
37. NPC-db2: Niemann-Pick Type C Database. Accessed January 24, 2017, at <https://medgen.medizin.uni-tuebingen.de/NPC-db2/index.php>.
38. Basu SK, Goldstein JL, Anderson GW, and Brown MS. 1976. Degradation of cationized low density lipoprotein and regulation of cholesterol metabolism in homozygous familial hypercholesterolemia fibroblasts. *Proc. Natl. Acad. Sci. USA.* **73**: 3178–3182.
39. Grosheva I, Haka AS, Qin C, Pierini LM, and Maxfield FR. 2009. Aggregated LDL in contact with macrophages induces local increases in free cholesterol levels that regulate local actin polymerization. *Arterioscler. Thromb. Vasc. Biol.* **29**: 1615–1621.
40. Havel RJ, Eder HA, and Bragdon JH. 1955. The distribution and chemical composition of ultracentrifugally separated lipoproteins in human serum. *T. J. Clin. Invest.* **34**: 1345–1353.
41. Ashkenas, J., M. Penman, E. Vasilie, S. Acton, M. Freeman, and M. Krieger. 1993. Structures and high and low affinity ligand binding properties of murine type I and type II macrophage scavenger receptors. *J. Lipid Res.* **34**: 983–1000.
42. Pipalia NH, Huang A, Ralph H, Rujoi M, and Maxfield FR. 2006. Automated microscopy screening for compounds that partially revert cholesterol accumulation in Niemann-Pick C cells. *J. Lipid Res.* **47**: 284–301.
43. Millard, E. E., K. Srivastava, L. M. Traub, J. E. Schaffer, and D. S. Ory. 2000. Niemann-pick type C1 (NPC1) overexpression alters cellular cholesterol homeostasis. *J. Biol. Chem.* **275**: 38445–38451.
44. Zhang, M., N. K. Dwyer, D. C. Love, A. Cooney, M. Comly, E. Neufeld, P. G. Pentchev, E. J. Blanchette-Mackie, and J. A. Hanover. 2001. Cessation of rapid late endosomal tubulovesicular trafficking in Niemann-Pick type C1 disease. *Proc. Natl. Acad. Sci. USA.* **98**: 4466–4471.
45. Nakasone, N., Y. S. Nakamura, K. Higaki, N. Oumi, K. Ohno, and H. Ninomiya. 2014. Endoplasmic reticulum-associated degradation of Niemann-Pick C1: evidence for the role of heat shock proteins and identification of lysine residues that accept ubiquitin. *J. Biol. Chem.* **289**: 19714–19725.
46. Watari, H., E. J. Blanchette-Mackie, N. K. Dwyer, M. Watari, E. B. Neufeld, S. Patel, P. G. Pentchev, and J. F. Strauss 3rd. 1999. Mutations in the leucine zipper motif and sterol-sensing domain inactivate the Niemann-Pick C1 glycoprotein. *J. Biol. Chem.* **274**: 21861–21866.
47. Dunn, K. W., and F. R. Maxfield. 1992. Delivery of ligands from sorting endosomes to late endosomes occurs by maturation of sorting endosomes. *J. Cell Biol.* **117**: 301–310.

48. Ghosh, R. N., D. L. Gelman, and F. R. Maxfield. 1994. Quantification of low density lipoprotein and transferrin endocytic sorting HEp2 cells using confocal microscopy. *J. Cell Sci.* **107**: 2177–2189.
49. Mukherjee, S., R. N. Ghosh, and F. R. Maxfield. 1997. Endocytosis. *Physiol. Rev.* **77**: 759–803.
50. Xu, W. S., R. B. Parmigiani, and P. A. Marks. 2007. Histone deacetylase inhibitors: molecular mechanisms of action. *Oncogene.* **26**: 5541–5552.
51. Dass, C. R., E. T. H. Ek, and P. F. M. Choong. 2007. Human xenograft osteosarcoma models with spontaneous metastasis in mice: clinical relevance and applicability for drug testing. *J. Cancer Res. Clin. Oncol.* **133**: 193–198.
52. Majumdar, A., E. Capetillo-Zarate, D. Cruz, G. K. Gouras, and F. R. Maxfield. 2011. Degradation of Alzheimer's amyloid fibrils by microglia requires delivery of ClC-7 to lysosomes. *Mol. Biol. Cell.* **22**: 1664–1676.
53. Lefevre, M. 1988. Localization of lipoprotein unesterified cholesterol in nondenaturing gradient gels with filipin. *J. Lipid Res.* **29**: 815–818.
54. Schwake, M., B. Schroder, and P. Saftig. 2013. Lysosomal membrane proteins and their central role in physiology. *Traffic.* **14**: 739–748.
55. Walczak, W., N. H. Pipalia, M. Soni, A. F. Faruqi, H. Ralph, F. R. Maxfield, and B. L. Webb. 2006. Parallel analysis of v-Src mutant protein function using reverse transfection cell arrays. *Comb. Chem. High Throughput Screen.* **9**: 711–718.
56. Freeman, M., Y. Ekkel, L. Rohrer, M. Penman, N. J. Freedman, G. M. Chisolm, and M. Krieger. 1991. Expression of type I and type II bovine scavenger receptors in Chinese hamster ovary cells: lipid droplet accumulation and nonreciprocal cross competition by acetylated and oxidized low density lipoprotein. *Proc. Natl. Acad. Sci. USA.* **88**: 4931–4935.
57. Deffieu, M. S., and S. R. Pfeffer. 2011. Niemann-Pick type C 1 function requires luminal domain residues that mediate cholesterol-dependent NPC2 binding. *Proc. Natl. Acad. Sci. USA.* **108**: 18932–18936.
58. Millard, E. E., S. E. Gale, N. Dudley, J. Zhang, J. E. Schaffer, and D. S. Ory. 2005. The sterol-sensing domain of the Niemann-Pick C1 (NPC1) protein regulates trafficking of low density lipoprotein cholesterol. *J. Biol. Chem.* **280**: 28581–28590.
59. Shi, Y., D. Gerritsma, A. J. Bowes, A. Capretta, and G. H. Werstuck. 2007. Induction of GRP78 by valproic acid is dependent upon histone deacetylase inhibition. *Bioorg. Med. Chem. Lett.* **17**: 4491–4494.
60. Yang, C., S. Rahimpour, J. Lu, K. Pacak, B. Ikejiri, R. O. Brady, and Z. Zhuang. 2013. Histone deacetylase inhibitors increase glucocerebrosidase activity in Gaucher disease by modulation of molecular chaperones. *Proc. Natl. Acad. Sci. USA.* **110**: 966–971.
61. Siegel, D., M. Hussein, C. Belani, F. Robert, E. Galanis, V. M. Richon, J. Garcia-Vargas, C. Sanz-Rodriguez, and S. Rizvi. 2009. Vorinostat in solid and hematologic malignancies. *J. Hematol. Oncol.* **2**: 31.